The Impact of Airflow on the Hygrothermal Behavior of Highly Insulated Pitched Roof Systems

Geert Houvenaghel **Arturo Horta, Ph.D.** **Hugo Hens, Ph.D.**
Member ASHRAE

ABSTRACT

Two important design parameters in insulated pitched roofs are (1) vapor-permeable versus vapor-tight underlays and (2) ventilated versus nonventilated roof constructions. In order to study the influence of both parameters on the hygrothermal performance, highly insulated pitched roof systems were constructed at the K.U.Leuven Vliet test building. During two years of testing, their hygrothermal response has been studied in detail. The roof eaves were redesigned between the first and the second year, with the main objective being to increase their wind-tightness.

The temperature and heat flux distributions show the importance of natural and forced air convection. The impact of air transfer shows that traditional thermal performance indicators, such as the conduction-related U-factor, no longer have a clear physical meaning. Measurements of the relative humidity fields, the moisture content in the rafters, and the occurrence of condensation confirmed the importance of air flow, not only for thermal but also for hygric performance. Air leakage measurements reveal the impact of minor perforations, with the leakage linked to the inside-outside temperature difference, wind direction, and wind speed. The air infiltration experiments show a clear relation between wind speed and direction and the magnitude and direction of the air flows in the roof sections.

The performance differences between the ventilated and the nonventilated roofs and between the roofs with a vapor-permeable underlay and those with a vapor-tight underlay are overshadowed by these air and wind flow effects. A comparison with previous test roof results also indicates that the very low density of the mineral wool used increases the importance of wind and air flow in and through the roof sections.

INTRODUCTION

In the United Kingdom nowadays, there is a tendency to incorporate the attic in the living space, which necessitates insulating the roof pitch instead of the ceiling. In continental Western Europe, insulated pitches have been common since the 1970s. In the 1970s and 1980s, many insulated pitched roof systems failed due to interstitial condensation. Hence, the following condensation control strategies were introduced: (1) adding a vapor retarder at the warm side of the insulation and (2) venting the air space between the underlay and the insulation. Since then, venting the underlay has been a subject of discussion.

Künzel and Grosskinksy (1989) show that a good airtightness of the roof pitches is a prerequisite in order to obtain any effect from underlay ventilation. Rose (2001) found that the effect of venting on the temperature of a shingle roof covering was rather limited. Hens and Janssens (1999) and Janssens and Hens (1999) showed that airtightness is needed in order to guarantee a correct hygric and thermal performance of pitched roofs, more than venting the underlay. Measurements by Derome (1998) confirmed that airtightness rather than ventilation is the key factor to prevent condensation problems. Also, ASHRAE (1997) and Rose (1995) focused on air leakage as an essential element in moisture control. Other researches agree that the effectiveness of a vapor retarder is

Geert Houvenaghel is Ph.D student and **Hugo Hens** is a professor and head, Laboratory of Building Physics, at Catholic University of Leuven, Belgium. **Arturo Horta** is technical manager at DuPont de Nemours Non-wovens, Luxembourg.

Table 1. Test Roof Classification

Test Roof	Ventilation	AFVR	Underlay
15-35 vented	Cavity under draped underlay, 50-25 mm	PE foil	Vapor-retarding bituminous felt, nonsealed overlaps
16-36 vented	Cavity under draped underlay, 50-25 mm	Spunbonded coated PP foil	Vapor-permeable Tyvek felt, nonsealed overlaps
17-37 compact	No	No	Vapor-permeable Tyvek felt, sealed overlaps
18-38 compact	No	Spunbonded coated PP foil	Vapor-permeable felt, sealed overlaps

reduced by air leakage but still advise to vent the underlay (Burch and Luna 1980; Liersch 1986). In the USA, much work dealing with these topics was done by Wilkes at ORNL.

Another subject of research is the use of vapor-permeable underlays. Künzel and Grosskinksy (1992) and Ojanen (2001) state that a vapor-permeable underlay may compensate for insufficient airtightness. Janssens (1998) shows that even with vapor-permeable underlays, a correct airtightness is needed.

This paper summarizes the research on pitched roofs in the Vliet test building at the Catholic University of Leuven (Belgium) during the winters of 2001-2002 and 2002-2003. The roof sections are representative of the British building tradition. The hygrothermal in-situ behavior of two vented and two compact roofs in a humid, moderate climate was analyzed in detail, focusing on the following topics:

- Compact versus ventilated
- Vapor-permeable versus vapor-retarding underlays
- Influence of an air flow and vapor retarder (AFVR)
- Influence of bad workmanship on hygrothermal performance

This paper focuses on the first two subjects.

TEST ROOFS

Roof Design

The study relates to four tiled wood-frame roof designs, typical of residential roof construction in Great Britain. All roofs contain the following layers (from the outside): (1) concrete tiles on laths and battens, (2) underlay foil, (3) 15 cm fiber glass insulation between rafters, and (4) painted gypsum board on battens. The use of an underlay foil as a protection for the insulation has become common practice in current residential construction.

The roofs differ in (1) the vapor permeability of the underlay, (2) the presence of a vented cavity between the underlay and the insulation, and (3) the type and presence of an AFVR at the inside of the insulation. Table 1 gives a classification of the four test roofs. Figure 1 shows the overall cross sections of the roofs. Table 2 lists the heat and air flow properties of the layers.

The design thermal properties of the test roofs are calculated on the basis of the measured thermal conductivities. The design thermal resistance of all roofs is equal to 4.6 m^2 K/W (26.12 h ft^2 °F/Btu), corresponding with a design U-factor of 0.2 W/m ^{2}K (0.04 Btu/h ft^2 °F).

After one winter, the eaves of all roofs were reconstructed in order to reduce the observed wind influence on the thermal performance of the roofs. Wind baffles were installed in the ventilated roofs in order to prevent wind penetrating the insulation material at the eaves (Houvenaghel and Hens 2004). In the compact roofs, the underlay was wrapped around the mineral fiber insulation in order to prevent unforeseen wind penetration.

Construction and Equipment

The field measurements were performed in the Vliet building, a test facility for the investigation of highly insulated envelope systems exposed to the outside climate (Janssens et al. 1995). The facility allows testing twenty wall systems, eight flat roofs and twelve pitched roofs simultaneously. The measuring bays are oriented northeast (15-16-17-18) and southwest (35-36-37-38). Southwest is the direction of prevailing wind and rain in Belgium and the direction with the highest incident solar radiation.

The test roofs are 1.8 m wide and 5.1 m long per pitch. The roof slope is 45°. The eaves of the vented roofs are detailed in order to enhance the flow of outside air into the cavity below the insulation. The vented roofs have a draped underlay foil with unsealed overlaps. In the compact roofs, the underlay is installed directly on top of the insulation, continuously from eave to eave, with a sealed overlap. All joints and intersections of the air flow and vapor retarder (AFVR) and the gypsum board are sealed in order to achieve a sufficiently low air permeance of the pitches. The measuring equipment consisted of (1) heat flux transducers applied at the inside of the gypsum board and of the underlay, (2) thermocouples at all material interfaces, (3) condensation indicators at the inside of the underlay, (4) moisture pins in the rafters, (5) relative humidity sensors at the inside of the underlay and the AFVR, and (6) pressure tubes at all material interfaces. All sensors are installed at three heights: at the eaves (450 cm form the ridge), in the middle of the roof, and at the top (95 cm from the ridge). The outside climate is monitored by a weather station located near the ridge at 10 m above ground level. The inside climate is monitored. All measuring and climatic sensors are continuously monitored on a 10-minute basis.

Roof 35-15
vented roof, AFVR, vapour retarding underlay

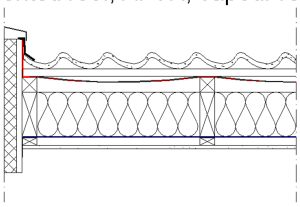

- concrete tiles
- underlay bituminous felt, draped, non-sealed overlaps
- vented cavity 25 to 50mm
- 15cm mineral fibre, between rafters 50x150mm
- HD PE AFVB,
- cavity 25mm
- gypsum board, triple coated with emulsion paint

Roof 36-16
vented roof, AFVR, vapour permeable underlay

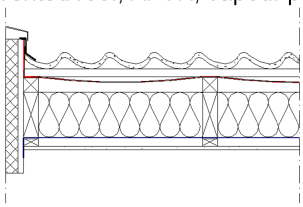

- concrete tiles
- vapour open underlay Tyvek, draped, non-sealed overlaps
- vented cavity 25 to 50mm
- 15cm mineral fibre, between rafters 50x150mm
- spunbonded AFVB,
- cavity 25mm
- gypsum board, triple coated with emulsion paint

Roof 37-17
compact roof, no AFVR, vapour retarding underlay

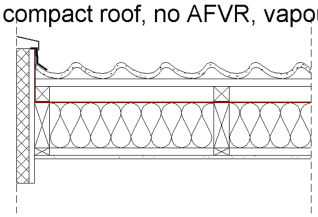

- concrete tiles
- vapour open underlay Tyvek, sealed overlaps
- 15cm mineral fibre, between rafters 50x150mm
- cavity 25mm
- gypsum board, triple coated with emulsion paint

Roof 38-18
compact roof, AFVR, vapour permeable underlay

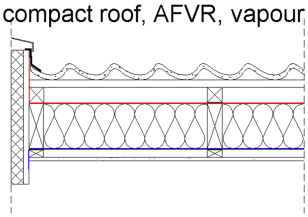

- concrete tiles
- vapour open underlay Tyvek, sealed overlaps
- 15cm mineral fibre, between rafters 50x150mm
- spunbonded AFVB,
- cavity 25mm
- gypsum board, triple coated with emulsion paint

Figure 1 *Cross section of the test roofs.*

Table 2 (SI). Measured Material Properties: Thickness *d*, Density, Thermal Conductivity λ, and Air Permeance K_a

Layer	d [mm]	Density	[W/m K]	K_a [m/s Pa] at Δp = 10 Pa
Vapor-permeable underlay	0.419	0.140 kg/m^2	-	28.59 10^{-7}
Bituminous felt	1.677	1.708 kg/m^2	-	5.44 10^{-7}
Mineral fiber insulation		9 kg/m^3	0.034	
Spunbonded AFVR	0.268	0.112 kg/m^2	-	5.00 10^{-7}
PE AFVR	0.281	0.268 kg/m^2	-	4.56 10^{-7}
Painted gypsum board	12.23	8.15 kg/m^2	R = 0.06 m^{2}K/W	6.86 10^{-7}

Table 2 (I-P). Measured Material Properties: Thickness *D*, Density, Thermal Conductivity λ, and Air Permeance K_a

Layer	d [inch]	Density	[Btu/s ft·°F]	K_a [m/s Pa] at Δp = 10 Pa
Vapor-permeable underlay	0.016	0.029 lb/ft^2	-	28.59 10^{-7}
Bituminous felt	0.066	0.350 lb/ft^2	-	5.44 10^{-7}
Mineral fiber insulation		0.562 lb/ft^3	0.55 10^{-5}	
Spunbonded AFVR	0.011	0.023 lb/ft^2	-	5.00 10^{-7}
PE AFVR	0.011	0.055 lb/ft^2	-	4.56 10^{-7}
Painted gypsum board	0.481	1.669 lb/ft^2	R = 0.34 h ft^2 ºF/Btu	6.86 10^{-7}

ENVIRONMENTAL CONDITIONS

Table 3 summarizes the outside environmental conditions for both winters. Winter 1 spans from October 2001 to March 2002, winter 2 from December 2002 to Mach 2003. During both winters, the outside climatic conditions were normal.

The interior climate is characterized by θ_i = 22.9°C (73.2°F) with a mean vapor pressure difference between inside and outside of 423 Pa (0.061 psi). That value corresponds to an indoor climate of class 3 (Hens 1992), representative for social dwellings.

THERMAL PERFORMANCE: VENTILATED VERSUS COMPACT

Heating Season Averages

Figure 2 gives the heating season averaged values of the heat fluxes at the underlay and at the inside of the gypsum board and the temperatures at the inside and outside of the insulation. Both the vented and the compact roofs show a nonuniform temperature and heat flux distribution. Solar radiation causes the heat fluxes through the underlay to be lower at the southwest than at the northeast pitch, and the temperatures of the underlay to be higher. The solar radiation effect is somewhat more pronounced in the compact roofs than in the vented roofs.

The vented roof has lower heat fluxes at the underlay than at the inner side of the insulation, which is typical for forced convection and wind washing. The temperature increases from the eaves to the ridge. These effects are more pronounced than for the compact roof since in the vented roof outside air may flow through the nonsealed overlaps of the underlay. Outside air penetrates at the eaves, which is reflected by the smaller temperature gradient across the insulation at the eaves. The heat flux and temperature distribution at the northeast pitch corresponds to a convectional air flow from eaves to ridge in the ventilation gap.

For the compact roofs, in both the southwest and the northeast pitch, the heat flux at the inner side of the insulation is higher in the middle than at the eaves and ridge. The inside temperature of the insulation in the middle of the southwest pitch, which is the windward pitch most of the time, is significantly lower. Since all gaps of the underlay are sealed in the compact roof, the major reason for the remarkable temperature and heat flux distribution may be rotational air flow in the insulation, corresponding to Benard cells (Bejan 1993). Figure 3 suggests, for that reason, the major air flow patterns that may develop in the ventilated and compact roofs. The number of rotation loops may be higher or lower than two.

Apparent and Local Equivalent R-Values

According to ASTM C1155 (ASTM 1995) the apparent local R-value is calculated as

$$R_{app,local} = \frac{\sum \Delta\theta}{\sum q}, \qquad (1)$$

where q = the measured daily averaged heat flux (W/m^2) at the inside of the gypsum board and $\Delta\theta$ = the measured daily averaged temperature difference (°C) between the inside of the gypsum board and the underlay. Table 4 gives the apparent local R-values for each position at each slope, the apparent R-value for the southwest and the northeast pitch, and the apparent equivalent R-value during the first winter. Table 5 gives the same results during the second winter.

Without infiltration or exfiltration, without air intrusion, and without rotation or wind washing, all measured R_{app} values should be the same, which is clearly not the case. The difference in apparent equivalent R-value between vented and compact roof is negligible, as is the influence of re-detailing the eaves between both winters.

The lowest apparent local thermal resistance is measured in the middle position for all orientations, both for the compact and the vented roofs, before as well as after re-detailing the eaves. The absolute minimum of all R_{app} values for the vented roofs is measured at the northeast middle position and for the compact roofs at the southwest middle position. For the vented roofs, the R_{app} values are higher at the southwest pitch than at the northeast pitch, except at the eaves. For the compact roofs the southwest R_{app} values are lower than the northeast R_{app} values, except at the eaves.

Table 3. Average Outside Environmental Conditions and Total Amount of Rain

			Winter 1	Winter 2
Temperature	q	[°C]	7.5 (45.5°F)	4.31 (39.8°F)
Relative humidity	RH	[%]	85.2	81.5
Vapor pressure	p_v	[Pa]	928.5 (0.135 psi)	786.5 (0.114 psi)
Wind velocity	v	[m/s]	1.9	1.8
Rain *		[mm]	533.8	218.6
Solar radiation		[kW/m^2]	0.329 (0.104 kBtu/h.ft^2)	0.257 (0.081 kBtu/h.ft^2)
*Some data are lacking				

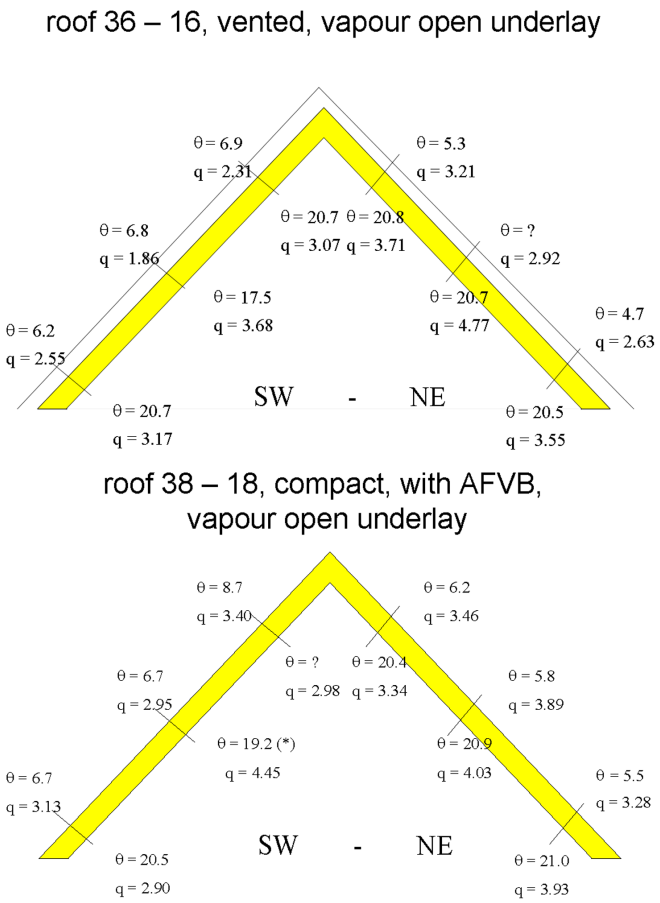

Figure 2 *Season heating averaged heat fluxes* q *at the underlay and the inside of the gypsum board; temperatures* θ *at the inside and outside of the insulation: (a) vented roof 36-16, (b) compact roof 38-18.*

In the vented roof the measured heat fluxes through the gypsum board are systematically higher than those through the underlay. Cold outside air enters the ventilation gap between the insulation and the underlay and transports heat as enthalpy to the outside. The heat flux and R_{app} distribution correspond to enthalpy transfer due to cavity ventilation, wind washing, or wind infiltration. For the compact roofs, the heat flux and R_{app} distribution are somewhat more diffuse.

Table 6 compares the heat loss measured through the underlay and through the gypsum board. When air exfiltration or infiltration and wind intrusion are absent, the heat losses through both surfaces should be equal. For the vented roofs, the heat flow through the underlay is significantly lower than that through the gypsum board. The difference is higher at the windward than at the leeward side. This indicates that ventilation really works. In the compact roof, in most cases, the heat loss at the inside is close to that at the outside. This illustrates how no longer external air infiltration or exfiltration or wind intrusion is the major air effect but rather internal air rotation. For all wind directions, the heat flow difference is higher for southwest than northeast.

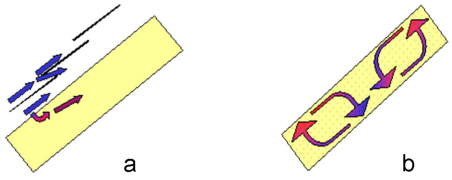

Figure 3 *Schematic representation of the main air flow patterns in (a) the vented roof and (b) the compact roof. Several rotation loops may occur in the compact roof.*

The observed thermal performance may be caused by two types of air flow:

- air looping in and around the insulation, due to temperature differences (natural convection, air rotation)
- air infiltration in and underneath the insulation, due to wind pressures (forced convection, wind washing)

Table 4 (SI). Apparent Local and Equivalent R-Values During the First Winter

R_{app}	Position	Area	Vented Roof 36/16		Compact Roof 38/18	
[m^2K/W]		[m^2]	SW pitch	NE pitch	SW pitch	NE pitch
R_{app} position	ridge	2.75	4.78	4.40	4.26	4.51
	middle	4.13	3.94	3.69	3.69	4.06
	eaves	1.76	4.74	4.96	5.06	4.20
R_{app} orientation			4.33	4.12	4.09	4.23
R_{app} global roof			4.22		4.16	

Table 5 (SI). Apparent Local and Equivalent R-Values During the Second Winter

R_{app}	Position	Area	Vented Roof 36/16		Compact Roof 38/18	
[m^2K/W]		[m^2]	SW pitch	NE pitch	SW pitch	NE pitch
R_{app} position	ridge	2.75	4.78	4.36	4.26	4.63
	middle	4.13	3.89	3.54	3.85	4.00
	eaves	1.76	4.83	4.88	5.14	4.17
R_{app} orientation			4.32	4.00	4.19	4.22
R_{app} global roof			4.15		4.21	

Table 4 (I-P). Apparent Local and Equivalent R-Values During the First Winter

R_{app}	Position	Area	Vented Roof 36/16		Compact Roof 38/18	
[h·ft^2·°F/Btu]		[ft^2]	SW pitch	NE pitch	SW pitch	NE pitch
R_{app} position	ridge	29.6	27.14	24.98	24.19	25.61
	middle	44.5	22.37	20.95	20.95	23.05
	eaves	18.9	26.91	28.16	28.73	23.85
R_{app} orientation			24.59	23.39	23.22	24.02
R_{app} global roof			23.96		23.62	

Table 5 (I-P). Apparent Local and Equivalent R-Values During the Second Winter

R_{app}	Position	Area	Vented Roof 36/16		Compact Roof 38/18	
[h·ft^2·°F/Btu]		[m^2]	SW pitch	NE pitch	SW pitch	NE pitch
R_{app} position	ridge	29.6	27.14	24.76	24.19	26.29
	middle	44.5	22.09	20.10	21.86	22.71
	eaves	18.9	27.42	27.71	29.18	23.68
R_{app} orientation			24.53	22.71	23.79	23.96
R_{app} global roof			23.56		23.90	

Table 6 (SI). Averaged Total Heat Flux Through the Underlay and the Gypsum Board During Winter 2

		SW pitch			NE pitch		
		$Q_{underlay}$	$Q_{gypsm\ board}$	ΔQ	$Q_{underlay}$	$Q_{gypsm\ board}$	ΔQ
Wind direction	**Roof type**	**[W]**	**[W]**	**[W]**	**[W]**	**[W]**	**[W]**
All	vented	18.80	29.77	10.97	25.74	36.26	10.52
	compact	27.16	31.90	4.75	31.57	32.90	1.33
SW	vented	16.49	28.48	11.99	24.17	30.67	6.50
	compact	25.14	29.25	4.11	27.93	29.26	1.34
NE	vented	22.34	31.79	9.54	28.14	45.05	16.89
	compact	31.10	36.00	4.90	37.24	38.65	1.42

Table 6 (I-P). Averaged Total Heat Flux Through the Underlay and the Gypsum Board During Winter 2

		SW pitch			NE pitch		
		$Q_{underlay}$	$Q_{gypsm\ board}$	ΔQ	$Q_{underlay}$	$Q_{gypsm\ board}$	ΔQ
Wind direction	**Roof type**	**[Btu/h]**	**[Btu/h]**	**[Btu/h]**	**[Btu/h]**	**[Btu/h]**	**[Btu/h]**
All	vented	64.1	101.6	37.5	87.8	123.7	35.9
	compact	92.7	108.8	16.1	107.7	112.2	4.5
SW	vented	56.3	97.2	40.9	82.5	104.6	22.1
	compact	85.8	99.8	14.0	95.3	99.8	4.5
NE	vented	76.2	108.5	32.3	96.0	153.7	57.7
	compact	106.1	122.8	16.7	127.1	131.9	4.8

The effect of both convection types on the thermal resistance can be expressed as

$$\frac{1}{R_{app,meas}} = \frac{1}{R_o} + C_1(\theta_{si} - \theta_{ul}) + C_2 v \cos(\alpha)\ , \qquad (2)$$

where $R_{app,meas}$ = the measured daily averaged apparent thermal resistance (m^2K/W), θ_{si} and θ_{ul} = the daily averaged temperatures (°C) at the inner surface and at the underlay, v = the daily averaged wind velocity (m/s), and α = the daily averaged angle between the wind direction and the normal direction on the roof shield. The constants R_o, C_1, and C_2 are determined from a multiple linear regression analysis. Only days with a daily averaged wind direction between southeast-southwest-northwest and with a daily averaged temperature difference $(\theta_{si}-\theta_{ul})>5$°C are taken into account in order to select data with the same wind orientation and thermal stack effect. Table 7 gives the results. When the relative error on the constants C_1 and C_2 is higher than 100%, the corresponding variable is not taken into account for the regression. A positive C_1 corresponds to increasing heat losses due to air looping. $C_2 > 0$ for southwest pitches and $C_2 < 0$ for northeast pitches correspond to increasing heat losses due to wind washing.

The regression results illustrate the following effects:

- The influence of air looping in the leeward northeast pitches is limited. The thermal performance of the windward southwest pitches is influenced by air looping: for each 10°C temperature difference, the energy losses increase by ±11% compared to the conductive heat losses.
- The thermal performance of the vented roof is strongly influenced by wind. At an average wind speed of 3 m/s, the heat losses increase about 25% at the windward side. At the leeward side, the heat losses increase by 28%.
- The thermal performance at the leeward side of the compact roof is hardly influenced by wind. At the windward side, the heat losses increase by 6% to 26% with a wind velocity of 3 m/s. The low overall correlation coefficients for the compact roofs indicate that the data show some scatter, which suggests that other effects may have more impact.

Wind Influence

In this section, the relation between the daily averaged wind speed and the measured daily averaged thermal performance is presented. In order to exclude uncertainties on the in-situ measurements, the measured thermal resistances are not directly used for the analysis. The ratio between the measured

Table 7. The Influence of Natural and Forced Convection on the Heat Losses at the Middle Position with SW Wind During Winter 2002-2003* (Measured at the Ridge)

Roof type	Pitch	R_o	$\sigma(R_o)$	C_1	$\sigma(C_1)$	C_2	$\sigma(C_2)$	R^2
		[m^2K/W]		[W/m^2K]		[$W\ s/m^3\ K$]		
Vented	SW	5.2	0.1	0.0025	0.0003	0.018	0.002	0.77
	NE (*)	5.3	0.2	0.0006	0.0003	-0.027	0.002	0.83
Compact	SW	5.4	0.7	0.0031	0.0012	0.022	0.005	0.43
	NE	4.3	0.1	0.0010	0.0004	-0.002	0.002	0.10

apparent thermal resistance for calm weather (limit at zero wind speed) to the apparent thermal resistance at the daily averaged wind speed is considered. This ratio is expressed by the Nusselt number (Nu) as given in Equation 3:

$$\mathrm{Nu} = \frac{R_0}{R_{1D,M}(v)} \tag{3}$$

where v = the wind speed (m/s), $R_{1D,M}$ = the measured one-dimensional apparent thermal resistance (m^2K/W), and R_0 = the measured one-dimensional apparent thermal resistance $R_{1D,M}$ at calm weather (v <1 m/s). The thermal resistance is calculated by Equation 1.

The Nusselt number is a measure of the increase of the heat losses through a roof due to wind washing. Nu >1 corresponds to an increase of the energy losses, Nu <1 means a decrease of the energy losses.

Figures 4 and 5 show the relation between the daily averaged Nu number and the daily averaged wind speed component $v_\perp$ perpendicular to the roof slope at different orientations for vented and compact roofs. The component $v_\perp$ is defined as

$$v_\perp = v\cos(\alpha_w - \alpha_n)\,, \tag{4}$$

where v = the wind speed (m/s), α_w = the wind direction (°, 0° = N, 90° = E], and α_n = the direction normal to the roof surface (°). This representation is preferred because the difference between the windward and the leeward pitch is more pronounced than when using the conventional averaged wind speed. Since southwest is the dominant wind direction, $v_\perp$ is most of the time positive for the southwest pitch and negative for the northeast pitch. Table 8 gives the reference thermal resistance R_0. The data at the middle position of the northeast vented roof are lacking due to a failure of the measurement sensors. The vented roof shows R_0-values that correspond well with the theoretical R-value of 4.6 W/m^2K, better than the heating season averaged apparent R-values given in Tables 4 and 5, which take into account data at all wind speeds and wind directions. The southwest pitch has a lower R_0 value than the northeast pitch. For the compact roof, the R_0 values are strongly dependent on the position and are mostly lower than the theoretical values. This is an indication of rotational air flow caused by natural convection in and around the thermal insulation.

Table 8 and Figures 4 and 5 show the following global effects:

- **Compact roofs.** The thermal performance of the compact roofs is more or less constant for all wind directions and wind speeds. At the leeward northeast pitch, hardly any wind effect is noticeable. For the southwest pitch, some extra heat losses are induced by southwestern wind. The influence is limited to 17% at the eaves and 22% in the middle of the roof at a wind speed v = 4 m/s. The thermal performance at the southwest ridge is not influenced by wind.
- **Vented roofs.** The southwest-facing vented roof shows a pronounced increase of heat loss with increasing wind speed when facing the wind. The wind influence increases from the eaves (+11% at v = 4 m/s) to the ridge (+37% at v = 4 m/s). In the middle of the roof, additional heat losses are induced by wind, both on the leeward- and the windward-facing roofs. Heat losses decrease with up to 30% at the southwest ridge when the southwest pitch is the leeward side; this is due to air flowing over the ridge from the northeast to the southwest pitch.
- The windward northeast pitchonly shows a minor increase of heat loss at increasing wind speed (19% at v = 4 m/s). At the northeast ridge, extra heat losses up to 39% are detected with southwest wind. This indicated that cold outside air enters at the northeast ridge even when the wind is blowing wouthwest.

The influence of wind on the thermal performance of the roofs may be explained by two possible phenomena:

- Intrusion of outside air in or beneath the insulation due to wind pressure gradients over the roof surface (wind washing). The increase of the wind influence from the eaves to the ridge is an indication of this phenomenon.
- Flow of internal or external air through the pitch due to wind-induced pressure differences across the roof shield: infiltration of outside air at the windward pitch, exfiltration of inside air at the leeward pitch.

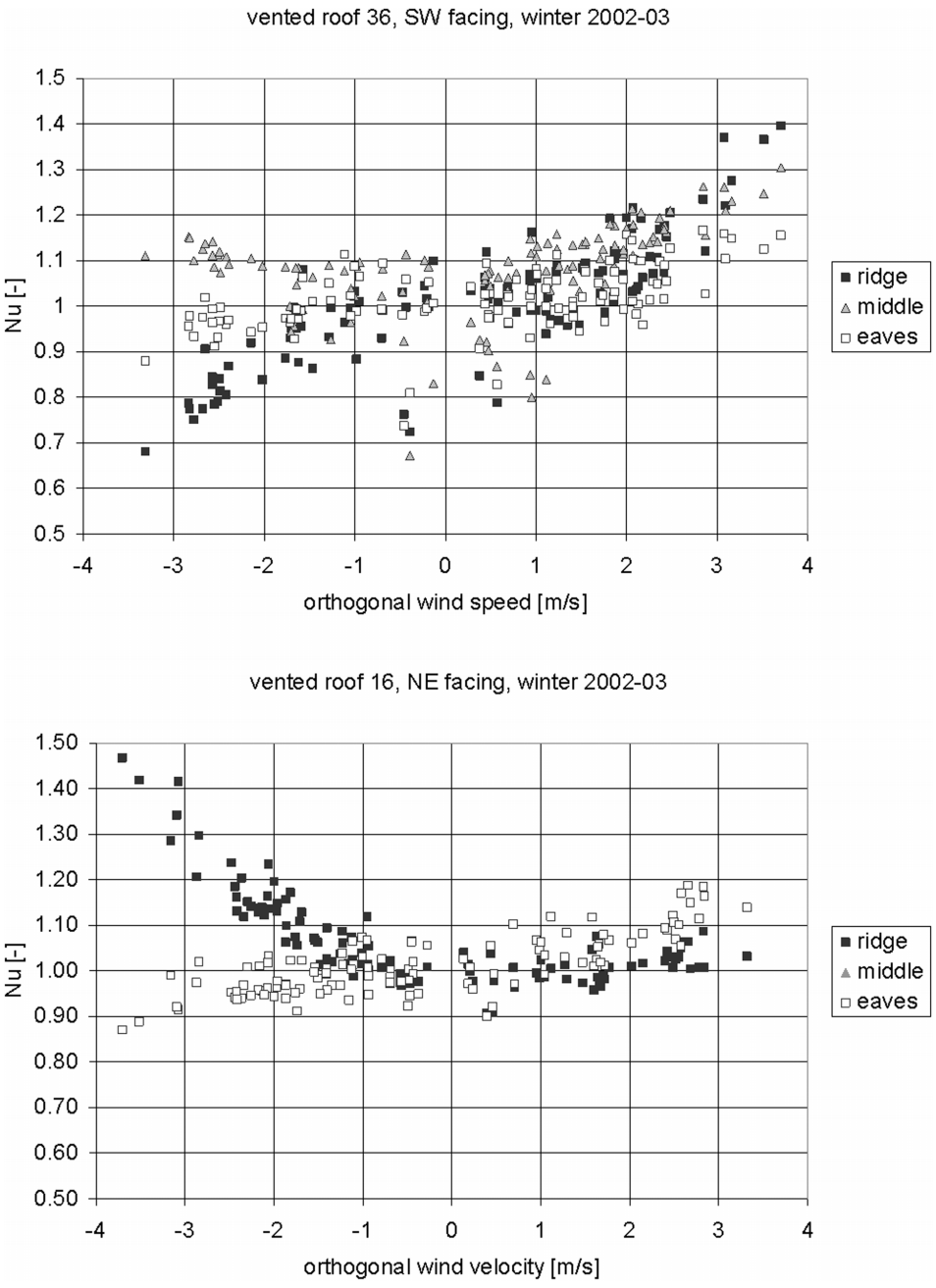

Figure 4 *Vented roof. Daily averaged Nusselt number versus wind speed orthogonal to the pitch.*

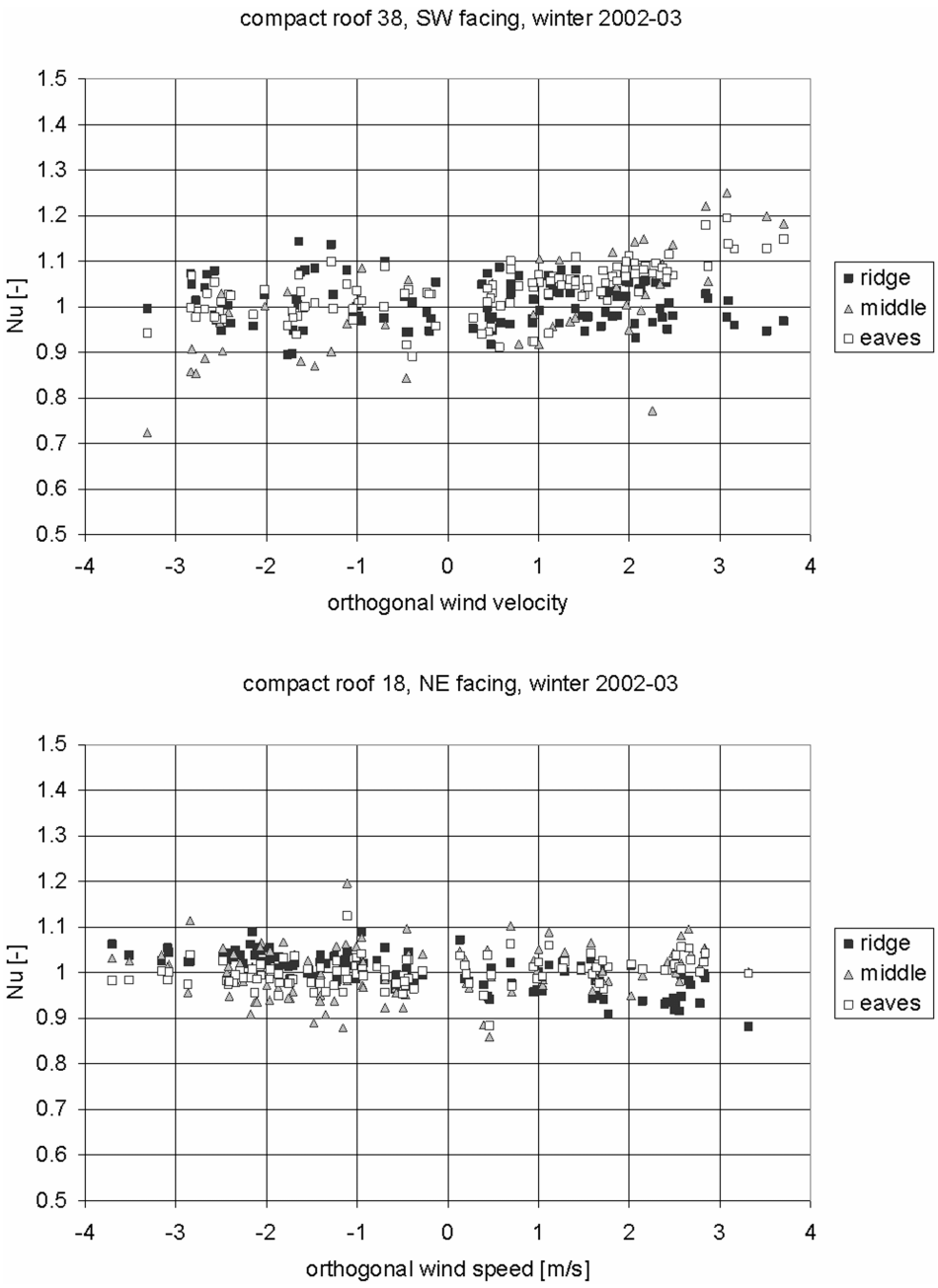

Figure 5 *Compact roof. Daily averaged Nusselt number versus wind speed orthogonal to the pitch.*

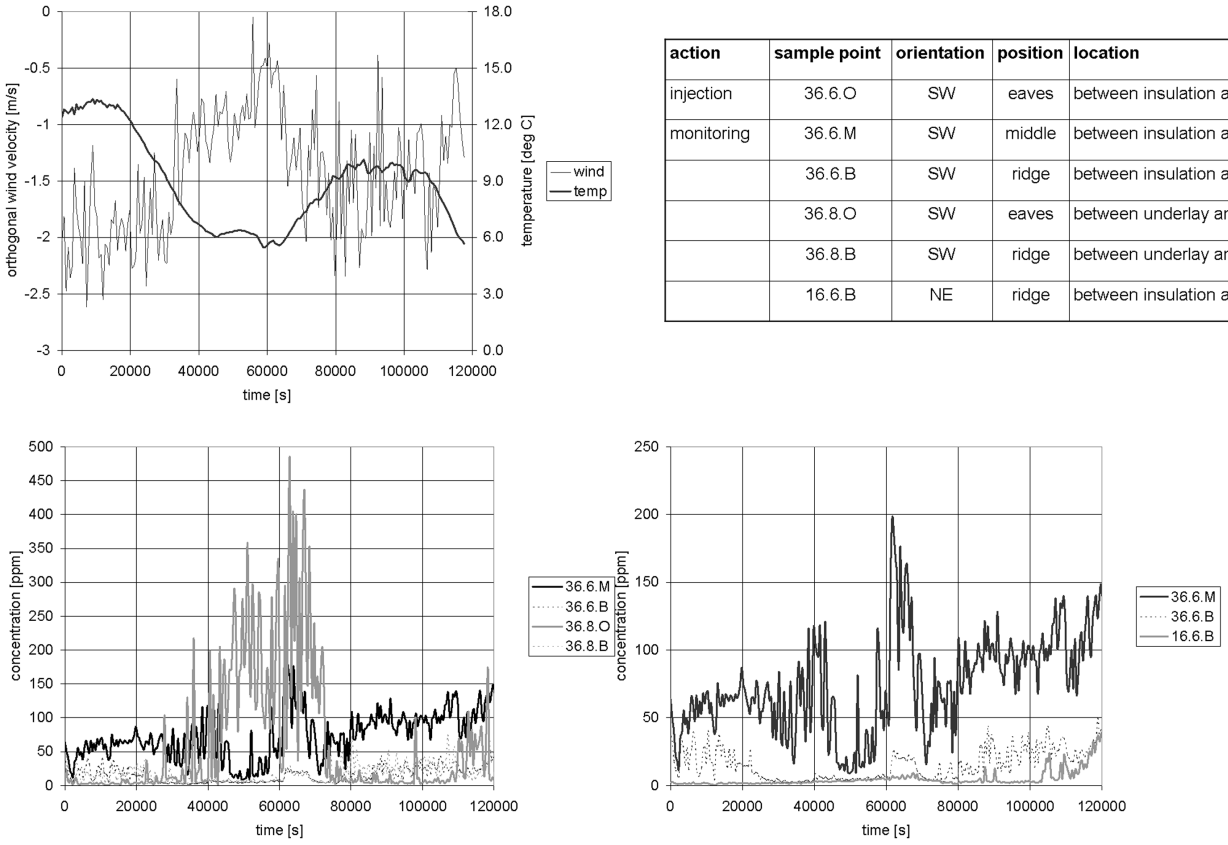

action	sample point	orientation	position	location
injection	36.6.O	SW	eaves	between insulation and underlay
monitoring	36.6.M	SW	middle	between insulation and underlay
	36.6.B	SW	ridge	between insulation and underlay
	36.8.O	SW	eaves	between underlay and tiles
	36.8.B	SW	ridge	between underlay and tiles
	16.6.B	NE	ridge	between insulation and underlay

Figure 6 *Air infiltration test on vented roof: climatic conditions and tracer gas concentrations.*

Table 8. Reference Thermal Resistance During Winter 2002-2003

R_0	Vented		Compact	
[m^2K/W] ([h ft^2 ºF/Btu])	SW	NE	SW	NE
Ridge	4.74 (26.91)	4.60 (26.12)	4.23 (24.02)	4.62 (26.23)
Middle	4.37 (24.81)	-- (--)	3.82 (21.69)	4.00 (22.71)
Eaves	4.88 (27.71)	4.91 (27.88)	5.30 (30.09)	4.17 (26.74)
Averaged	4.58 (26.01)	4.72 (26.80)	4.18 (23.73)	4.22 (23.96)

Verification of Air Intrusion and Air Exfiltration/Infiltration

Two tracer gas techniques were applied to determine the dominant air flow patterns in the roofs in a quantitative way. The first technique evaluates the airtightness of the roofs. During the test a constant tracer concentration is maintained in the test building while the migration of gas into to the different roof cavities is monitored simultaneously. The second technique studies the movement of air within the roof cavity of one single roof. Tracer gas is dosed at a constant rate at a certain point of the roof, and the migration of the gas to other sample points in the roof is measured. The tracer gas used is SF_6.

Figure 6 shows a typical result of the second measuring technique on the vented roof 16-36. During the measurement the wind was blowing northeast with an average velocity v = 1.8 m/s. The average outside temperature was 8.9 ºC. The tracer gas is injected between the insulation and the underlay at the eaves of the southwest pitch, which is oriented leeward. Figure 6b shows the measured tracer concentration at the middle and the ridge of the southwest pitch and the ridge of the northeast pitch. The southwest concentrations are strongly fluctuating as a function of time, which is an indication of wind influence. Figure 6c shows the measured tracer concentrations at the inside and outside of the underlay. The measurements reveal the following.

- At average wind velocities, the stack effect seems to be the driving force for cavity ventilation in the leeward roof shield, illustrated by the more or less logarithmic concentration built up for the middle position between the insulation and the underlay. The ridge shows a similar behavior but at a much lower concentration level. This can be due either to external air flowing from the northeast to the southwest pitch over the ridge or to external air intruding between the underlay overlaps. The strong concentration fluctuations indicate that external air intrusion is occurring.
- At low wind velocities, during the night period, the concentration between the underlay and insulation drops to nearly zero at the ridge. At the middle position, the concentration shows an irregular profile, and strongly fluctuating concentrations are measured between the tiles and the underlay at the eaves. When the wind velocity increases, this concentration drops to zero due to a higher outside air flow in the cavity above the underlay. This illustrates that outside air can easily penetrate at the underlay overlaps.
- The concentration at the ridge is similar above and beneath the underlay: outside air can penetrate or exfiltrate via the underlay overlaps.

Figure 7 shows the results of a tracer experiment on the compact roof with a west wind of 2 m/s and an outside temperature of 15°C. The tracer is injected between the insulation and the underlay in the southwest eaves, which are oriented windward. The concentrations at the inner side of the insulation are nearly constant, while those at the outer side show a more erratic behavior. The latter indicates wind influence. All concentrations at the inner and the outer side of the insulation are nearly similar. This distribution corresponds to air rotation around the insulation. The concentration at the inner side of the insulation at the eaves is remarkably higher than the others, illustrating that the insulation is very air permeable. Supposing an ideal tracer mixing, the concentration profile illustrates that separate air rotation loops are formed and that, even if air intrusion is less important for the compact roof, it still is present.

The results of the air tightness test on the compact roofs with and without AFVR are shown in Figure 8. The concentrations between the insulation and the underlay result from equilibrium between inside air at the room concentration and outside air at a zero concentration infiltrating the roof. The inside air flow is determined by the overpressure of the building and the airtightness of the roof and may as such be considered constant during the test. The outside air flow depends on the quality of the underlay and the environmental conditions and varies mainly with the wind velocity. From the measurements, several conclusions can be made:

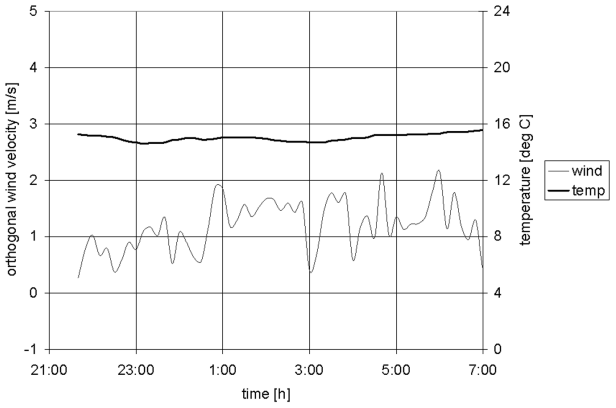

action	sample point	orientation	position	location
injection	38.7.O	SW	eaves	between insulation and underlay
monitoring	38.4.O	SW	eaves	between AFVR and insulation
	38.4.M	SW	middle	between AFVR and insulation
	38.4.B	SW	ridge	between AFVR and insulation
	38.7.M	SW	middle	between insulation and underlay
	38.7.B	SW	ridge	between insulation and underlay

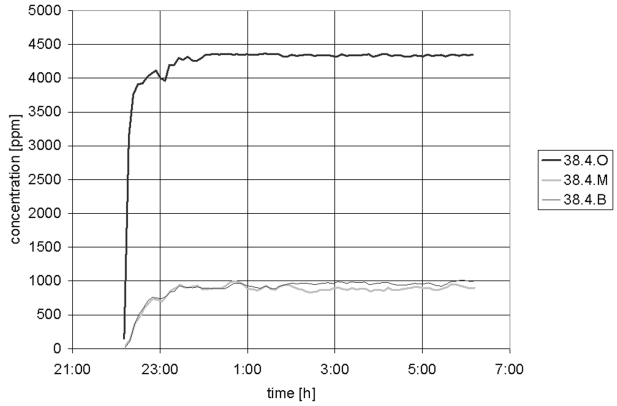

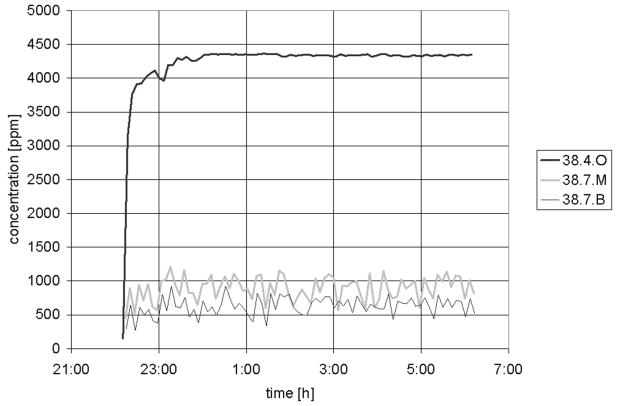

Figure 7 *Air infiltration test on the compact roof (38): climatic conditions and tracer gas concentrations.*

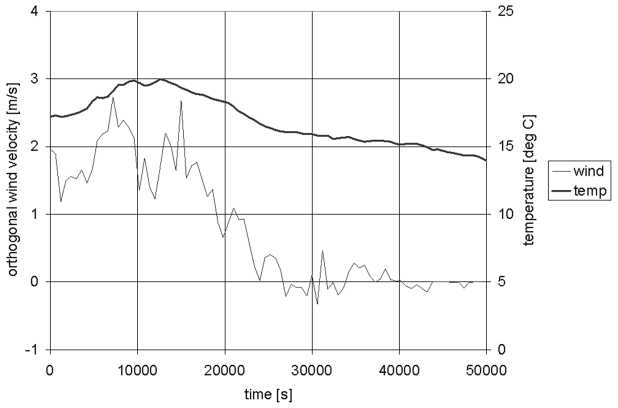

action	sample point	orientation	position	location
injection	room			inside test building
vented	37.4.M	SW	middle	between gypsum board and insulation
	37.7.M	SW	middle	between insulation and underlay
Compact	38.2.M	SW	middle	between gypsum board and AFVR
	38.4.O	SW	eaves	between AFVR and insulation
	38.7.M	SW	middle	between insulation and underlay

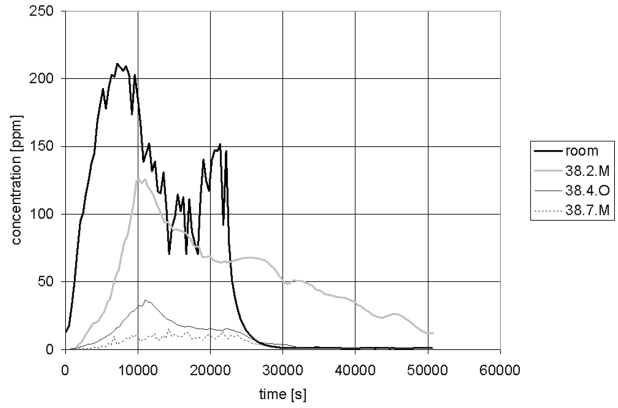

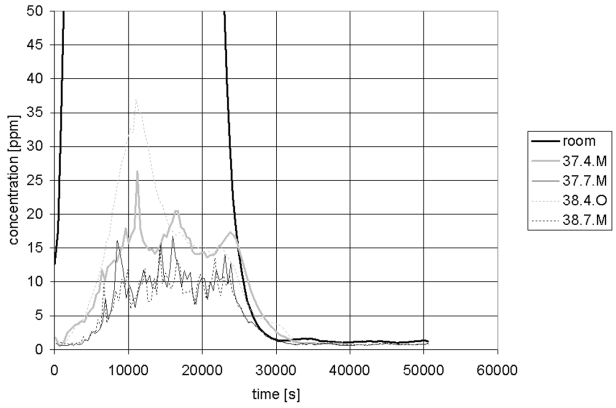

Figure 8 *Air leakage experiment on the compact roof without an AFVR (37) and with an AFVR (38).*

- None of the roofs is perfectly airtight.
- Painted gypsum board is a good air flow retarder as long as it is not perforated. The gypsum board of the compact roof with an AFVR was perforated for measurement reasons, although the perforation was sealed as well as possible, due to which the airtightness of the gypsum board dropped.
- The AFVR is effective in that the slope of the concentration buildup is lower at the outside of the foil.
- The concentrations between the underlay and the insulation are similar for the compact roof with an AFVR and the compact roof without an AFVR, due to the airtightness of the gypsum board.

The measured concentration differences can be due to differences in air exfiltrating from the test building (G_{ex}) as well as to differences in cavity ventilation or outside air infiltration (G_{in}). The ratio between the exfiltrating and the infiltrating air flow can be calculated. Figure 9 shows a clear relation between the wind velocity and the air flow rate. For wind velocities higher than 0.5 m/s, the air exfiltration is only a fraction of the outside air infiltration, both in the vented and the compact roof. Therefore, the only valuable explanation for the observed wind dependency of the thermal performance of the vented and compact roofs can be intrusion of outside air in, through, and under the thermal insulation (wind washing). Similar conclusions have been found for wood-frame insulation constructions (Ojanen 1996; Uvsløkk 1996) and pitched roofs (Janssens et al. 1998).

Discussion of Results

The temperature profiles do not significantly differ between the vented and the compact roof with an AFVR. The measured heat fluxes show that air flow plays an important role in both roofs: in the vented roofs, air intrusion and wind washing are major effects, while in the compact roofs, internal air rotation is the dominant phenomenon. These air and wind influences lower the apparent thermal resistance over a heating season by 9% from what is theoretically expected.

There is no significant difference in overall average energy performance measured between the vented and the compact roofs. The fact that both the vented and the compact roof have more or less the same overall thermal performance is due to wind and air flow and strongly related to the low density of the mineral fiber insulation used (Lecompte 1989). Janssens et al. (1998) showed that the energy performance of

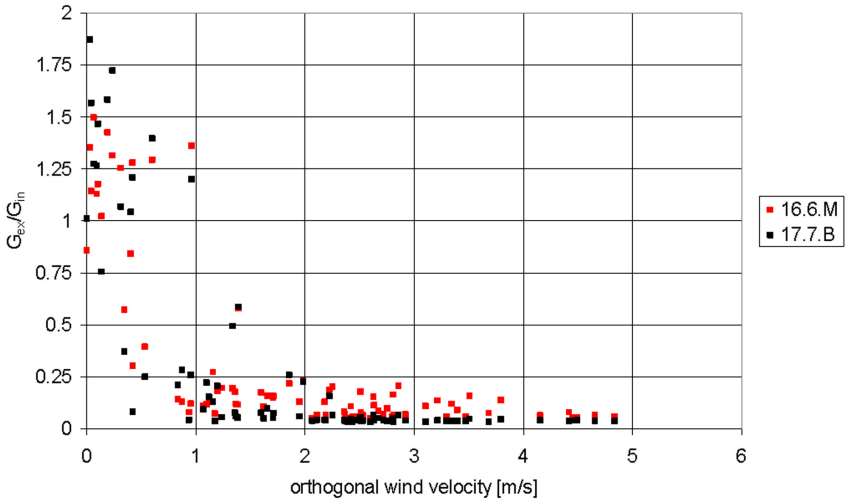

sensor	roof	orientation	position	location
16.6.M	vented roof	NE	middle	between AFVR and insulation
17.7.B	compact roof without AFVR	NE	ridge	between tiles and underlay

Figure 9 *Ratio between the inside air exfiltration flow and the cavity outside air ventilation flow as a function of wind velocity.*

compact roofs is better than that of vented roofs due to less air intrusion and wind washing effects when mineral wool with a higher density (18.4 kg/m^3 or 1.15 pounds/ft^3) is used.

MOISTURE PERFORMANCE

Introduction

This section of the paper deals with the moisture performance of the test roofs. The major moisture sources in pitched roofs are (1) rain, (2) built-in moisture, (3) the inside relative humidity, and (4) the outside relative humidity.

In the test roofs the underlay foils ended in a small gutter in order to measure the amount of rainwater penetrating the tiles and running off the underlay. No water was collected in these gutters; no rain penetration was observed. Since all wood was protected from rain during construction, the built-in moisture was negligible in the test roofs.

Interstitial condensation and the wetting-drying balance of the roofs is evaluated by studying:

- the measured RH underneath the underlay and below the insulation
- the measured condensation indications by the condensation sensors

The measured data are compared with the calculated condensation and drying potentials of the inside and the outside air.

Relative Humidity and Vapor Pressure

Table 9 gives the statistical distribution of the measured daily average relative humidity (RH) underneath the underlay. The 10th percentile gives the relative humidity value under which the relative humidity drops during 10% of the time. When interpreting the data, one should take into account that due to condensation the relative humidity sensor may give results higher than 100%. The differences in relative humidity can mostly be explained by temperature differences (warmer is dryer). The major conclusions are:

- The relative humidity in the southwest pitches is lower than in the northeast ones.
- During winter the relative humidity is higher in the compact roofs than in the vented roofs. During summer the relative humidity in the compact roofs is similar or even lower than in the vented roofs.
- The compact roof without an AFVR foil has a higher relative humidity at the windward slope during winter than the one with an AFVR. At the leeward northeast pitch, the relative humidity is significantly higher in the compact roof with an AFVR.
- When studying the frequency of RH = 100%, we can conclude that at the windward side, the vented roofs show the highest relative humidity in the middle position. The compact roofs have the highest at the ridge. At the leeward side, the distribution is more diffuse. The compact roofs showed a higher number of RH = 100% events than the vented roofs. This could be due to the drying capacity of outside air, which can enter by the overlaps over the whole pitch length in the vented roofs.

Table 9. Daily Averaged Relative Humidity Underneath the Underlay: Average Value, 10% and 90% Values

	Ridge			Middle			Eaves		
	10%	**50%**	**90%**	**10%**	**50%**	**90%**	**10%**	**50%**	**90%**
	NE pitches								
15	77.1	96.0	100	85.5	100	100	63.6	88.4	100
16	70.6	90.6	100	-	-	-	63.3	80.6	93.1
17	84.1	100	100	78.3	91.1	98.3	78.7	92.1	98.9
18	76.1	100	100	80.6	92.9	98.2	75.6	86.5	92.2
	SW pitches								
35	67.0	84.3	95.0	67.4	84.0	95.4	73.3	90.2	100
36	41.0	55.2	63.5	65.3	88.1	98.7	61.0	72.3	78.4
37	72.5	97.2	100	72.2	86.7	96.8	71.2	85.5	95.5
38	68.8	83.7	93.6	76.8	98.3	100	70.7	84.7	95.5

Measurements of the relative humidity underneath the insulation did not show major differences between the compact and the vented roofs, except from temperature-related differences in relative humidity.

Whereas the relative humidity should always be interpreted taking the temperature into account, the vapor pressure is a real thermodynamic variable. Figure 10 compares the vapor pressures in the vented and the compact roofs with the inside and outside vapor pressure. The following may be concluded.

- All measured vapor pressures correspond better to the outside than to the inside vapor pressure. This shows that the moisture-control strategy of using an AFVR at the warm side of the insulation is working well. A non-perforated, painted gypsum board may act as an AFVR.
- The vapor pressure underneath the underlay is slightly higher in the compact roofs than in the vented roofs. At the ridge the vapor pressure is slightly higher in the compact roof without an AFVR than in the compact roof with an AFVR.
- The same observations are made underneath the insulation.

Interstitial Condensation: Condensation and Drying Potentials

Condensation and moisture accumulation in roof constructions are only possible if there is a moisture source from which vapor can migrate into the roofs. Both the inside and the outside air can act as a moisture source. Condensation is only possible when the dew point of the inside or outside air is higher than the surface temperature of one of the material layers in the roof, i.e., when the vapor pressure exceeds the saturation vapor pressure at one of the material surfaces. Whether or not condensation will really occur under these circumstances depends on the vapor resistance between the surface and the air and on the drying-wetting balance at the material surface.

The difference between the vapor pressure in the air and the saturation vapor pressure on the material surface is an important boundary condition when evaluating the condensation risk of a construction. We define the condensation potential *CP* between the air and a certain surface as

$$CP = p - p_{sat}(\theta_s) , \qquad (5)$$

where p = the vapor pressure of the air (Pa) and p_{sat} = the saturation vapor pressure on the surface (Pa). Since the saturation vapor pressure is a function of the surface temperature θ_s (°C), the outside air can only act as a moisture source when the surface is undercooling with respect to the outside temperature. Undercooling is due to radiant heat exchange with the clear sky.

Table 10 gives the statistical data for undercooling and the condensation potentials on a 10-minute basis for the inside and the outside air at the tiles and the underlay. For each parameter the period of undershooting or exceeding the zero value and the values of the 10th and 90th percentile are given.

From Table 10 the following may be concluded.

- During winter the instantaneous surface temperature of the tiles is lower than the outside temperature. Due to solar radiation, the tiles of the southwest pitches show less undercooling. The underlay foils have a lower undercooling percentage time. Their temperature exceeds the air temperature by about 1°C. The undercooling time also depends on the type of roof: the vented underlays have a longer undercooling time and a lower average temperature than those in the compact roofs.
- The average condensation potential of the outside air is rather limited—only 22% of the time at the underlay. This means that during most of the time, drying of the underlay foils to the outside air is possible.

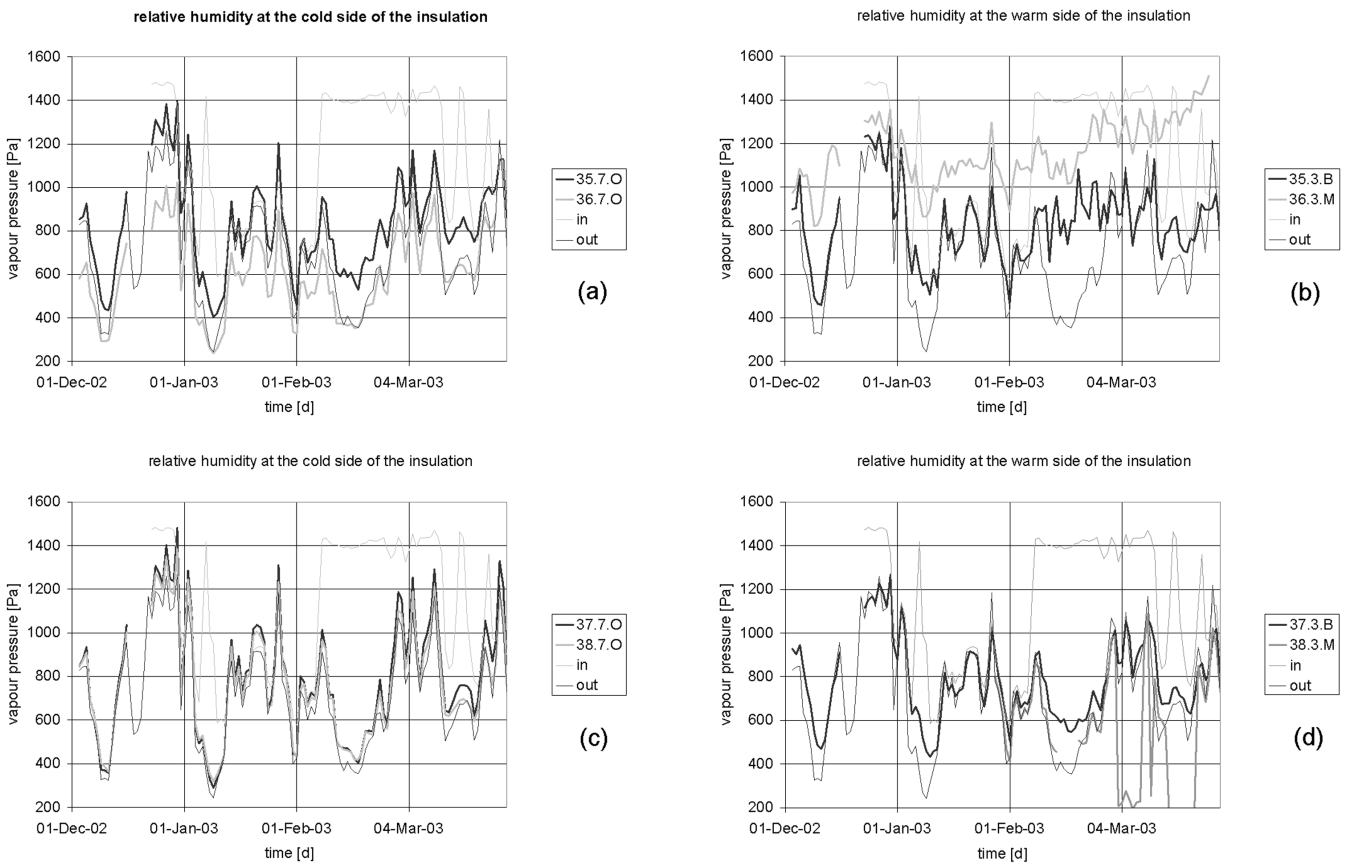

Figure 10 *Vapor pressures measured in the vented (35-36) and the compact (37-38) roofs compared with the inside and the outside vapor pressure: (a) gives the vapor pressure measured at the warm side of the insulation in the vented roofs, (b) gives the vapor pressure measured at the cold side of the insulation in the vented roofs, (c) gives the vapor pressure measured at the warm side of the insulation in the compact roofs, (d) gives the vapor pressure measured at the cold side of the insulation in the compact roofs. (O) eaves, (M) middle, (B) ridge.*

- We remark that in some roofs the undercooling and condensation potentials strongly vary with the position, which corresponds to the measured temperature profiles.

Interstitial Condensation: Condensation Indicators

The occurrence of interstitial condensation against the underside of the underlay foils is registered by means of condensation indicators (three for each roof shield). These condensation indicators produce an electrical signal when water vapor is condensing on them. The indicators give information about the time of wetness, not about the amount of condensate, and start reacting at high RH, lower than 100%. Figure 11 shows the measured condensation indicator signals for some pitches. In order to obtain a quantitative measure, the condensation indication is integrated over the measurement period (Figure 12).

The difference between vented and compact roofs is rather small. The difference between vapor-permeable and vapor-tight underlays is rather limited, too. These observations correspond well with the RH and vapor pressure measurements, which neither indicated severe condensation problems nor major differences between the vented and compact roofs and the different types of underlay. The major reason is that the outside condensation potential is rather limited for all roofs and that all roofs have a good air flow and vapor-retarding layer at the inside. Due to the latter and to wind intrusion, the hygric behavior of the roofs is completely determined by the outside environmental conditions and not by the inside condensation potential.

Recently some measurement bays have been installed in the roofs in order to open the underlay layer of each roof at a position near the ridge without introducing extra air and wind leakage. Under the underlay in the measurement opening, a blotting paper is installed to absorb the amount of condensation that is determined gravimetrically on a weekly basis. Measurements over last winter revealed a maximum moisture content of the blotting paper of 12 g/m^2 (0.0025 lb/in.^{2}). This is much lower than the critical amount of condensation of

Table 10. Statistical Distribution of Undercooling and the Inside and Outside Condensation Potential at the Tiles and the Underlay

			Undercooling			CP outside air			CP inside air		
			$\theta_s - \theta_e$			$p_e - p_{sat}(\theta_s)$			$p_i - p_{sat}(\theta_s)$		
			%<0	10%	90%	%>0	10%	90%	% >0	10%	90%
15	tile	Middle	75.0	-3.4	1.5	34.1	-545.7	110.0	75.3	-190.2	886.9
	UL	Ridge	42.2	-1.5	3.5	9.4	-712.0	-3.8	65.7	-310.0	776.4
	UL	Middle	49.9	-2.0	2.7	14.9	-654.7	33.7	68.4	-272.1	814.7
	UL	Eaves	34.3	-1.4	2.7	19.2	-566.7	135.6	65.2	-308.8	768.4
16	tile	Middle	70.3	-2.8	1.2	26.8	-540.5	88.2	73.6	-213.3	878.5
	UL	Ridge	50.6	-1.9	2.9	14.4	-654.5	25.0	67.9	-289.8	822.8
	UL	Eaves	50.5	-1.9	1.9	20.9	-479.3	145.6	70.6	-231.7	801.2
17	UL	Ridge	39.7	-1.5	3.2	6.5	-685.7	-22.0	66.3	-286.6	771.8
	UL	Middle	38.2	-1.4	2.7	6.3	-611.2	-22.3	66.1	-259.0	776.3
	UL	Eaves	44.7	-1.5	2.2	20.2	-497.2	127.6	67.8	-245.9	791.1
18	UL	Ridge	33.9	-1.2	3.5	5.6	-698.8	-27.0	62.8	-322.3	772.3
	UL	Middle	40.6	-1.6	2.6	9.6	-597.5	-1.9	65.7	-294.2	791.9
	UL	Eaves	40.2	-1.5	2.2	20.4	-511.5	134.0	65.7	-290.1	787.8
35	UL	Ridge	18.1	-0.4	8.3	1.9	-1327.1	-66.4	55.0	-674.7	729.1
	UL	Middle	37.5	-1.4	6.9	9.6	-1137.2	-4.0	60.0	-518.1	776.8
	UL	Eaves	32.2	-1.0	4.9	19.6	-744.2	165.1	60.2	-356.2	747.4
36	tile	Eaves	82.7	-15.6	2.1	58.6	-516.0	795.5	79.0	-319.6	1019.7
	UL	Ridge	50.3	-1.8	6.3	12.8	-1059.9	19.6	64.6	-470.8	812.2
	UL	Middle	46.3	-1.5	5.1	10.2	-920.0	1.6	64.3	-368.6	790.0
	UL	Eaves	36.8	-1.1	4.2	20.4	-683.8	165.9	62.7	-327.7	766.4
37	tile	Middle	53.5	-6.65	7.1	34.3	-868.6	267.0	69.3	-338.1	851.8
	UL	Ridge	43.3	-5.0	8.1	25.4	-973.3	194.7	62.3	-432.8	776.5
	UL	Middle	45.5	-5.4	7.8	27.1	-911.5	205.9	63.8	-391.9	793.3
	UL	Eaves	40.9	-5.1	7.6	32.9	-769.8	336.0	61.2	-370.1	768.8
38	UL	Ridge	8.8	0.1	6.8	1.1	-1115.7	-115.1	53.1	-558.0	677.2
	UL	Middle	46.5	-1.7	5.1	11.8	-924.4	13.0	64.4	-404.6	805.5
	UL	Eaves	34.3	-1.2	4.2	21.8	-698.8	164.2	62.1	-363.5	770.6

200 g/m^2 (0.410 lb/in.^{2}) (Janssens 1998) and is only somewhat higher than the hygroscopic moisture content of the blotting paper (8 g/m^2 or 0.00016 lb/in.^{2} at 86% RH).

Discussion of Results

None of the roofs show major condensation problems. The moisture control strategy of an airflow-retarding layer at the inside and a vapor-open underlay or a vented underlay works properly. When the inside is airtight, the moisture performance of the roofs is dominated by the outside weather. Undercooling is the major source of condensation.

Painted nonperforated gypsum board acts as a good AFVR. Nevertheless, adding an extra AFVR foil at the inside of the insulation is not redundant since the gypsum board is often perforated in reality, and sealing perforations is nearly impossible.

The vented roofs show a somewhat lower relative humidity than the compact roofs, although no major differences in condensation behavior are noticed. From a thermal point of view, compact roofs are to be preferred since the impact of wind washing is lower than in vented roofs. This, however, is only fully true if the mineral fiber thermal insulation has a high enough density (≥ 18 kg/m^3 for glass fiber [Lecompte 1989]).

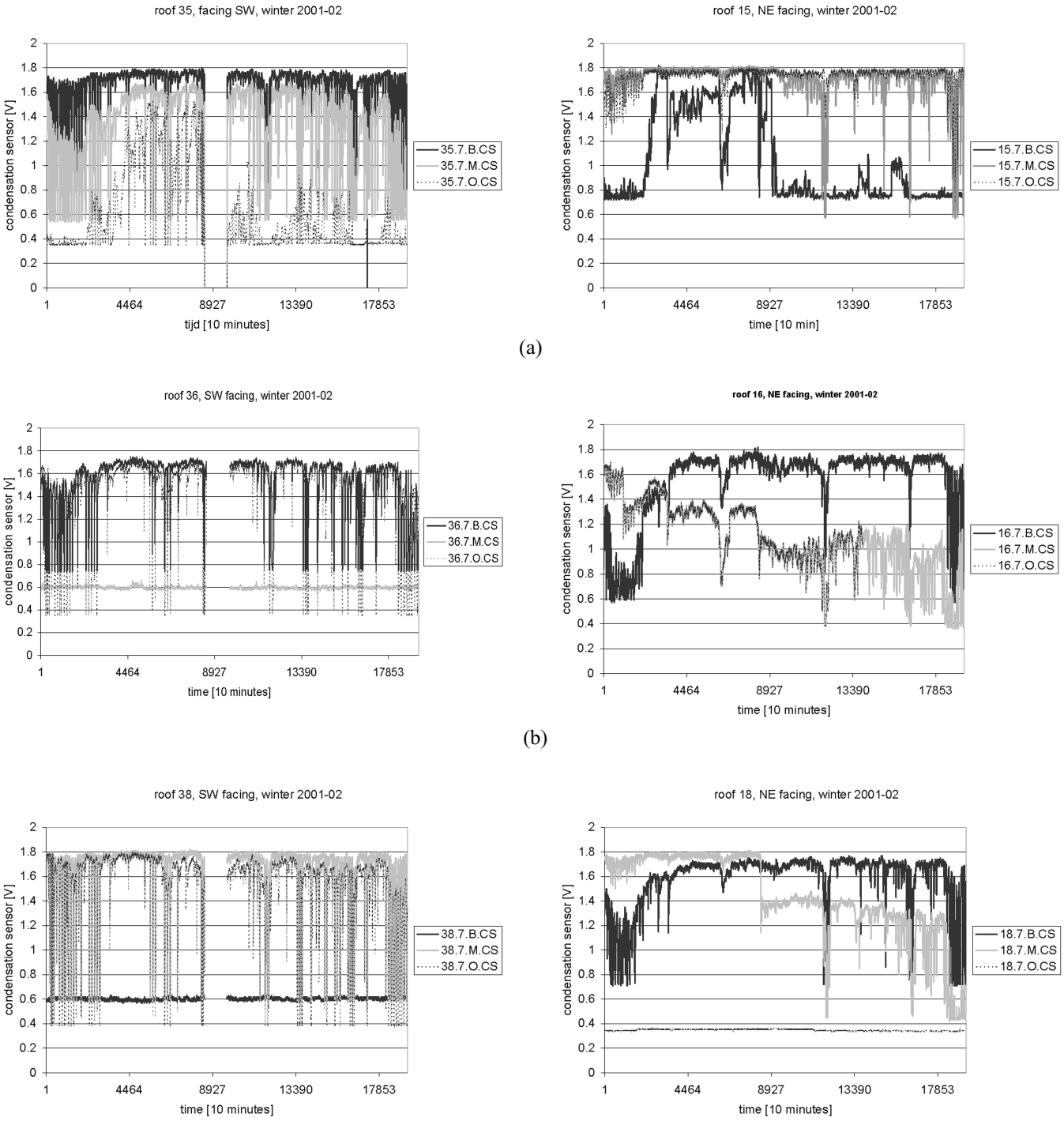

Figure 11 *Condensation indicators in (a) the vented roof 35-15 with a vapor-tight underlay, (b) the vented roof 36-16 with a vapor-permeable underlay, and (c) the compact roof 38-18 with a vapor-permeable underlay. Northeast pitches are given at the right-hand side, southwest pitches at the left-hand side. (B) bridge, (M) middle, and (O) eaves.*

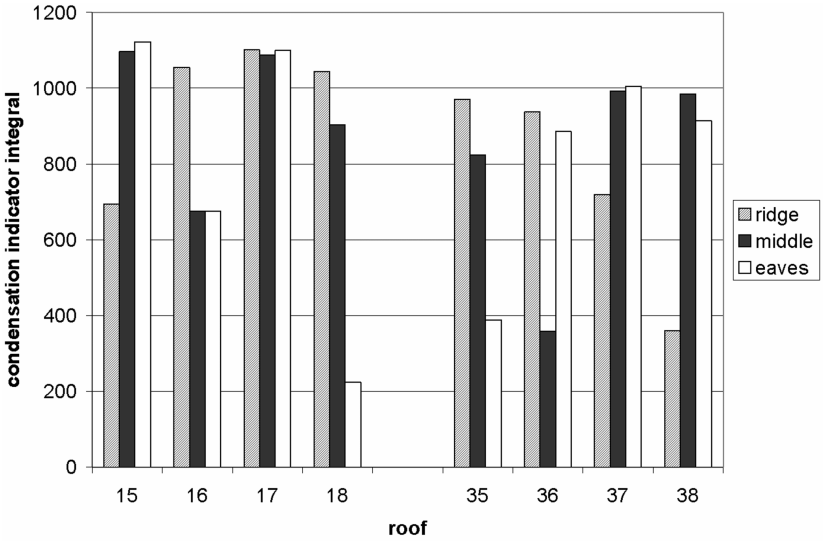

Figure 12 *Normalized integral of the condensation indicator over time, winter 2001-2002.*

SUMMARY, CONCLUSIONS, AND RECOMMENDATIONS

This paper presented measured results of the thermal and hygric performance of duo-pitched tiled wood-frame roof designs in a moderate, humid climate. The measurements showed that the thermal performance may be affected considerably by wind washing in the vented roofs and to a lesser extent in the compact roofs and by air rotation in the compact roofs when low-density mineral wool is applied as insulation material. The magnitude of the wind effect depends mostly on the orientation of the pitch relative to the wind direction. Between vented and compact roofs and roofs with and without an AFVR, not much difference was measured. This is mainly due to the low density of the mineral fiber insulation used, the good airtightness, and the difficulty of completely avoiding wind washing. The measurements nevertheless indicate that the current use of underlay foils with unsealed overlaps and mineral fiber insulation of too low density may jeopardize the desired quality of tiled roofs in building practice.

A nonperforated, painted gypsum board acts as an AFVR. Nevertheless, in practice, the use of an AFVR foil is recommended since the gypsum board layer is mostly perforated. The control strategy of using an AFVR layer at the inside of the insulation, in combination with a vapor-permeable underlay or a vented cavity, works well: the inside climate hardly has any impact on the hygric and condensation behavior of the roofs, which are dominated only by the outside environmental conditions. When undercooling of the underlay would be more severe, the use of a vapor-permeable underlay may be useful since drying to the exterior climate is favoured.

ACKNOWLEDGMENT

We would like to thank the DuPont de Nemours Nonwovens for their financial support and research interest.

REFERENCES

ASHRAE. 1997. *1977 ASHRAE Handbook—Fundamentals*. Atlanta: American Society of Heating, Refrigerating and Air-Conditioning Engineers, Inc.

ASTM. 1995. *ASTM Standard C1155, Standard practice for determining thermal resistance of building envelope components from in-situ data*. Annual Book of ASTM standards. American Society for Testing and Materials.

Bejan, A. 2004. *Convection heat transfer*. New York: Wiley.

Burch, D.M., and D.E. Luna. 1980. A mathematical model for predicting attic ventilation rates required for preventing condensation on roof sheeting. *ASHRAE Transactions* 86(1): 201-220.

Derome, D. 1998. Testing of flat roofs insulated with cellulose fiber. *Thermal Performance of the Exterior Envelopes of Buildings VII*. Atlanta: American Society of Heating, Refrigerating and Air-Conditioning Engineers, Inc.

Hens, H. 1992. Indoor climate classes. Internal Report IEA-Annex 24 T2-B-92/02, International Energy Agency. Heat air and moisture transfer in insulated envelope parts (HAMTIE), Laboratory of Building Physics, KULeuven, Belgium.

Hens, H., and A. Janssens. 1999. Heat and moisture response of vented and compact cathedral ceilings: A test house evaluation. *ASHRAE transactions* 105(1): 837-850.

Houvenaghel, G., and H. Hens. 2004. Pitched roofs with a vapour permeable underlay. Research Report, Laboratory of Building Physics, KULeuven, Belgium.

Janssens, A., H. Hens, and S. Roels. 1995. Vliet test building. Laboratory of Building Physics, KULeuven, Belgium.

Janssens, A., W. Depraetere, A. Morel, and H. Hens. 1998. Third annual report on the Vliet test building, Laboratory of Building Physics, KULeuven, Belgium (in Dutch).

Ojanen, T. 1996. Criteria for the hygrothermal performance of wind barrier structures. *Proceedings of the 4th Symposium on Building Physics in the Nordic Countries*, *VTT Building Technology, Espoo, Finland*, pp. 643-652.

Janssens, A. 1998. Reliable control of interstitial condensation in lightweight roof systems. Calculation and assessment methods. Ph.D. dissertation, Laboratory of Building Physics, KULeuven, Belgium.

Janssens A., and H. Hens. 1999. Thermal effects of windwashing in duo-pitches tiled roofs. *Proceedings of the 5th symposium of Building Physics in the Nordic Countries*, *Goteborg, Sweden*, pp. 417-424.

Lecompte, J. 1989. The influence of natural convection on the thermal quality of insulated cavity constructions. Ph.D. dissertation, Laboratory of Building Physics, KULeuven, Belgium (in Dutch).

Künzel, H., and T. Grosskinksy. 1989. Untersuchungen über die Feuchteverhältnisse bei w:armegedämmten Sateteldachkonstruktionen. FB25/1989, Fraunhofer Institut für Bauphysik, Holzkirchen, Germany (in German).

Künzel, H., and T. Grosskinksy. 1992. Vorteile diffusionaoffener, unbelüfteter Satteldachkonstruktionen. FB39/1992, Fraunhofer Institut für Bauphysik, Holzkirchen, Germany (in German).

Liersch, K.W. 1986. *Belüfte dach- und Wandkonstruktionen, Band 3: Dächer: Bauphyiskalische Grundlagen des Wärme- und Feuchteschutzes*. Wiesbaden-Berlin: Bauverlag (in German).

Ojanen, T. 2001. Thermal and moisture performance of a sealed cold roof system with a vapor-permeable underlay. *Thermal Performance of the Exterior Envelopes of Buildings VIII*. Atlanta: American Society of Heating, Refrigerating and Air-Conditioning Engineers, Inc.

Rose, W.B. 1995. The history of attic ventilation regulation and research. *Thermal Performance of Exterior Envelopes of Buildings VI*, pp. 379-390. Atlanta: American Society of Heating, Refrigerating and Air-Conditioning Engineers, Inc.

Rose, W.B. 2001. Measured summer values of sheating and shingle temperatures for residential attics and cathedral ceilings. *Thermal Performance of the Exterior Envelopes of Buildings VIII*. Atlanta: American Society of Heating, Refrigerating and Air-Conditioning Engineers, Inc.

Uvsløkk, S. 1996. The importance of wind barriers for insulated timber frame constructions. *J. Thermal Insul. and Bld. Envs*. 20 (July 1996): 40-62.